

1

Direct Conversions of Methane via Homogeneous Processes

Hui Chen, Anhua Hu, Liang Chang, Qing An, Hui Pan, and Zhiwei Zuo

ShanghaiTech University, School of Physical Science and Technology, 393 Middle Huaxia Road, Shanghai 201210, China

1.1 Introduction

Natural gas is typically viewed as a clean energy fuel and an economical chemical feedstock by the chemical community. With dwindling oil supplies and the growing importance of reducing the worldwide dependence on petroleum-based chemical products, the recent discovery of unconventional reservoirs with large volumes has made it an economically attractive raw material. In addition to the direct economic gain from the making of value-added chemical products, the upgrading of natural gas into liquid chemicals also could help reduce the capital and emission costs of the long-range transportation of natural gas. With more and more countries and societies committing to carbon neutrality in the forthcoming years, the development of innovative and effective means of utilizing this abundant natural resource for more sustainable chemical production has become urgent.

Methane is the main chemical component of natural gas, and thus, the direct transformation of methane into high-value liquid commodity chemicals has attracted enormous amounts of research attention across the scientific community over the past few decades [1–8]. Nevertheless, the central challenge of methane functionalization lies in its low intrinsic reactivity. The homolytic bond dissociation energy (BDE) of the C—H bonds in methane is 105 kcal/mol, which is the highest among all of the alkanes, indicating that methane is the least reactive light alkane [9]. In addition, because of methane's high ionization potential of 12.6 eV, electron affinity of 1.5 eV, high pK_a of 50 in dimethyl sulfoxide (DMSO), and proton affinity of 132 kcal/mol, direct conversions of methane involving electron transfer and proton transfer are unfavorable. Besides, the gaseous property of methane leads to its low solubility in most reaction solvents (e.g. methane has a 1 mM solubility in water at 1 atm and 25 °C), which renders the reaction concentration of methane in solution disadvantageous. Moreover, the introduction of any functional groups can result in more activated C—H bonds in the products, so unique selectivity for the methane C—H bonds has to be achieved. Despite these challenges, tremendous

progress has been made in the C–H functionalization of methane using transition metal catalysts such as Pt, Pd, and Hg [9]. Nevertheless, the practical demands of industrial development have imposed severe challenges on the utilization of coeffective catalysts and reagents and on ecologically benign conditions for the development of highly efficient and selective C(sp³)–H bond functionalizations, constantly driving the development of catalytic strategies.

In this chapter, we summarized the advancements in the direct conversion of methane through a homogeneous process. Notably, tremendous progress has been achieved in the heterogeneous research field [10–12], and it has been well-documented elsewhere; therefore, it is not included here. To further highlight the practical significance of homogenous catalytic platforms in methane C–H functionalizations, meanwhile covering the theoretical aspect of the eminent strategies for methane C–H activations, this chapter is categorized based on the type of products derived from the direct functionalization of methane, including methanol and its derivatives, acetic acid, methanesulfonic acid (MSA), aminated products, alkylated products, and borylated products (Figure 1.1).

1.2 Formation of Methanol and Its Derivatives

Methanol is a versatile commodity chemical, transportation fuel, and a promising energy carrier. With more than 20 million tons produced annually, methanol is mainly produced industrially from synthetic gas. In the past decades, significant research effort has been dedicated to developing a method for the direct oxidation of methane into methanol and its derivatives with the goal of obviating multistep and energy-intensive processes [13]. The central challenge lies in the low intrinsic reactivity of methane in comparison to activated C–H bonds of methanol (96 kcal/mol). Consequently, the conversion of methane and the selectivity of oxidative products have become important factors affecting the reaction efficiency, and overoxidation has to be suppressed to a large extent. Despite the significant challenges, tremendous progress has been achieved in the last 40 years. In this section, we divided the selected examples into two parts based on the activation modes of the methane: the transition metal-catalyzed electrophilic activation of methane into M–CH₃ species, the radical-mediated activation of methane through hydrogen atom transfer (HAT) into a methyl radical intermediate.

1.2.1 Electrophilic Activation

The C(sp³)–H bond of methane can be activated by a weak coordination with certain transition metal centers, namely electrophilic activation. More specifically, this activation strategy consists of two steps: the metal ion of complexed with C(sp³)–H bond of methane in an electrophilic fashion, the formed metal–methane complex could undergo oxidation and reductive elimination to generate the C–H functionalization products. These efficient metal catalysts for methane oxidation are expected to be relatively soft and easy to polarize and highly electrophilic species that can form

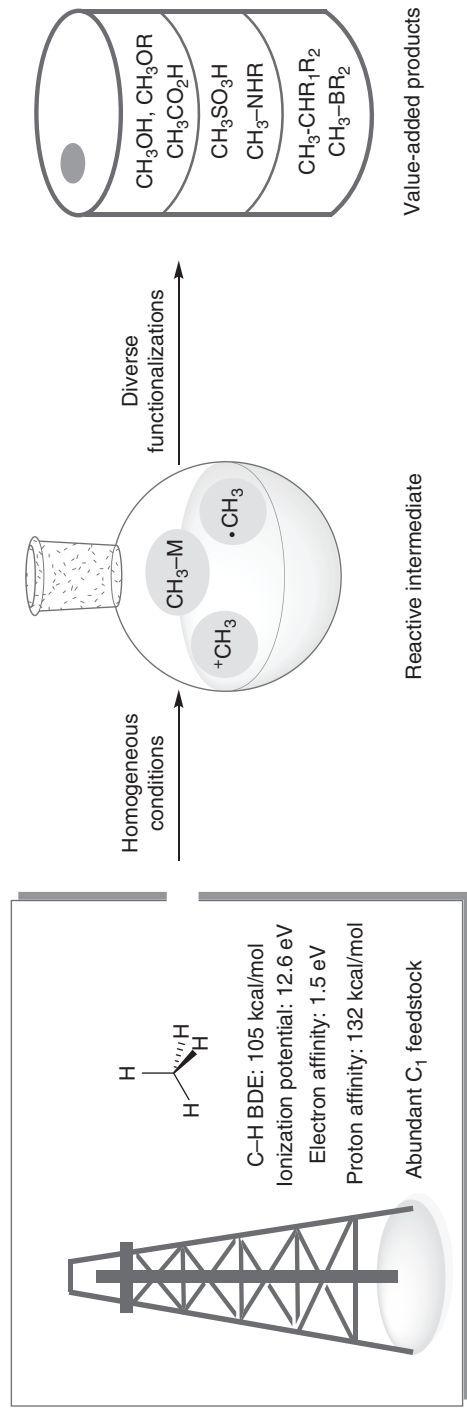


Figure 1.1 Direct conversions of methane via homogeneous processes.

relatively strong covalent bonds with carbon atoms are also good oxidants. Moreover, owing to the activated C—H bonds in methanol and its derivatives, highly acidic media such as oleum and trifluoroacetic acid are usually required for ensuring a high selectivity.

In the early 1980s, Shilov et al. reported the K_2PtCl_4 catalyzed direct conversion of methane into methanol for the first time [14, 15]. Employing K_2PtCl_6 as the oxidant at the relatively mild conditions, this reaction exhibits good selectivity for the generation of methanol product. A catalytic cycle of this approach was proposed in Figure 1.2. The activation of C—H bonds of methane by $(H_2O)_2PtCl_2$ species affords a Pt(II)— CH_3 intermediate, which is then oxidized to a high-valent Pt(IV)— CH_3 species by K_2PtCl_6 . Reductive elimination of the Pt(IV)— CH_3 intermediate yields the methanol product and regenerates the catalyst. This method opens up new avenue for the electrophilic activation of methane via a homogeneous process; however, the characteristics of low turnover frequency (TOF, $<10^{-5} s^{-1}$ at $<100^\circ C$), low turnover number (TON, <20), stoichiometric use of K_2PtCl_6 , and the distribution of oxidation products render this method inefficient in some degree.

In 1998, Periana et al. reported a platinum-catalyzed direct oxidation of methane into the methyl ester [16]. The 2,2'-bipyrimidine (bpym) ligand used in this reaction plays a crucial role to prolong the catalyst life and further improve the TONs. They

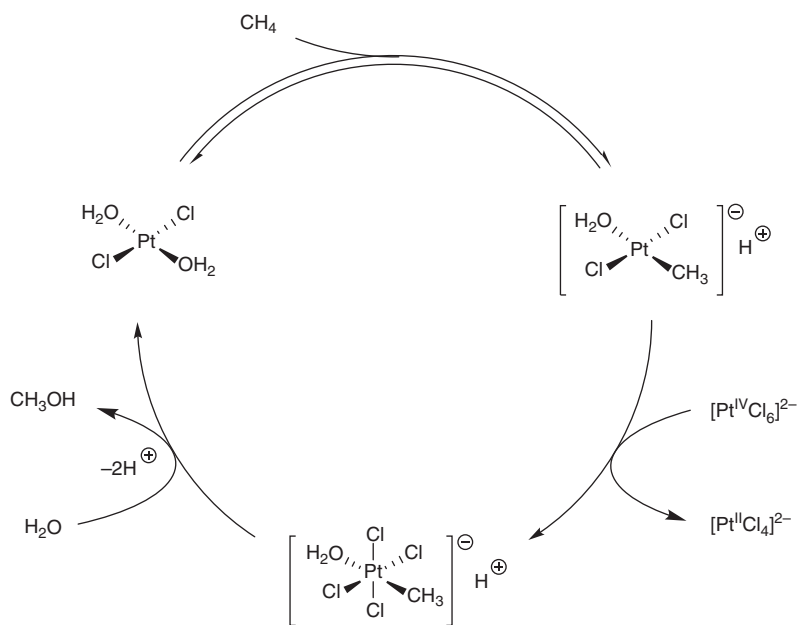
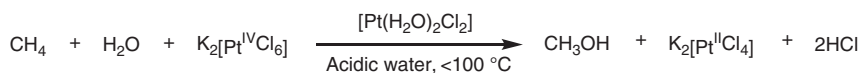


Figure 1.2 Catalytic oxidation of methane in Shilov reaction.

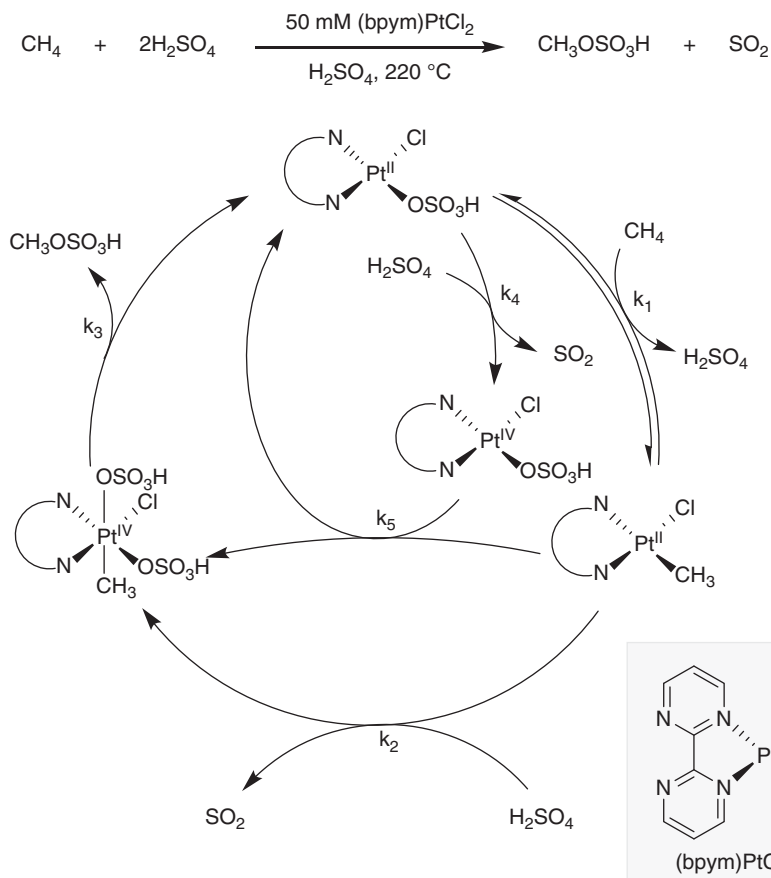


Figure 1.3 Modification of the Shilov reaction with (bpym)PtCl₂ complex. Source: Modified from Mironov et al. [17].

found that the (bpym)PtCl₂ complex is beneficial to increase the conversion of methane by up to 90% and the selectivity by about 81% at 220 °C in concentrated sulfuric acid, with methyl bisulfate as the major product. In comparison to the K₂PtCl₄, the (bpym)PtCl₂ catalyst is able to circumvent the formation of Pt black. Consequently, the TONs of the reaction are up to 300 with the TOF is about 10⁻³ s⁻¹. As depicted in Figure 1.3, a catalytic cycle of this catalytic system was proposed [17]. Initially, the electrophilic activation of methane by the active (bpym)Pt(II) forms a (bpym)Pt(II)-CH₃ species (step k₁). Then, the (bpym)Pt(II)-CH₃ species could either reduce the (bpym)Pt(IV) intermediate into the active (bpym)Pt(II) via a self-repair reaction (step k₅) or be transformed into (bpym)Pt(IV) species by the oxidation with H₂SO₄ (step k₂). Finally, reductive elimination of the (bpym)Pt(IV) species generates the methyl bisulfate product (step k₃).

Nevertheless, the activity of (bpym)PtCl₂ catalyst is highly sensitive to water and even a small amounts of water in this reaction system would cause diminished activity. In order to obtain the high conversion and efficiency, high catalyst loading

is required. Moreover, as the reaction generates water continuously, the TOF decreases sharply to $<10^{-5} \text{ s}^{-1}$ when the concentration of H_2SO_4 drops below 90%. To overcome this problem, additional SO_3 is needed to prevent the water accumulation through the incorporation of water into H_2SO_4 . Thusly, the concentration of H_2SO_4 remains above 98% throughout the oxidative process.

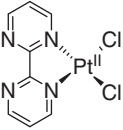
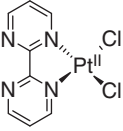
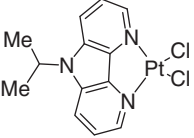
The separation of methanol from the reaction mixture is difficult because at least two volume equivalents of water are required to dilute the highly acidic system, resulting in the increased cost. Michalkiewicz et al. developed a low-pressure membrane distillation technique to separate the methyl bisulfate from the reaction mixture [18]. Schüth and coworkers investigated the crucial factors for selective oxidation of methane to methyl bisulfate with platinum salts [19–21]. They found that the use of (bpym)PtCl₂ in 20% oleum can effectively increase the TOF and selectivity (Table 1.1). Moreover, different catalysts have been found effective to enhance the electron density of the Pt center to achieve a higher catalytic activity. The screening result discloses that simple platinum salt K₂PtCl₄ is superior to the (bpym)PtCl₂ catalyst, with TOFs of up to 25 000 h⁻¹ and TONs of greater than 16 000 in 20% oleum. Later, Lee and coworkers introduced a (DMSO)₂PtCl₂-catalyzed methane oxidation to generate methyl bisulfate in oleum system [22]. Comparing with (bpym)PtCl₂ and K₂PtCl₄ catalysts, (DMSO)₂PtCl₂ catalyst exhibited an enhanced catalytic activity regarding both the yields and the TONs of methyl bisulfate. Under a catalyst concentration of 3.0 mM, the yield of methyl bisulfate reaches 84% with 94% selectivity. Besides, the TONs can be improved to 19 000 at the low catalyst concentration.

In addition to Pt(II) catalysts, other transition metal salts such as Hg(II) [23, 24] and Au(I) or Au(III) [25, 26] were also demonstrated to be effective catalysts for the oxidation of methane into methanol or methyl ester in highly acidic media, such as concentrated sulfuric acid or H₂SeO₄. However, the catalytic efficiencies are somewhat inferior to that obtained in Pt(II)-catalyzed systems (Table 1.2).

Generally, the electrophilic activation of methane by these catalysts is restricted in acidic media similar to or stronger than $\text{H}_2\text{SO}_4/\text{SO}_3$ at high temperatures in terms of the catalytic activity and catalyst solubility. Consequently, a more reactive catalyst is required in catalytic reactions employing much weaker acidic media such as acetic acid and trifluoroacetic acid. Sen and coworkers reported a Pd(II)-catalyzed oxidative of methane to methyl trifluoroacetate with trifluoroacetic acid as the solvent [27, 28]. This approach utilizes Pd(O₂CC₂H₅)₂ as the catalyst and H₂O₂ as the oxidant, methyl trifluoroacetate, could be obtained within 30 minutes at 90 °C. Whereas the low TON of about 5 is obtained, this Pd catalyzed system represents a successful example of methane activation under relatively weakly acidic conditions at a low temperature.

Strassner and coworkers have demonstrated *N*-heterocyclic carbenes (NHC) as effective ligands for Pd(II) to activate the methane [29, 30]. They found that solutions of Pd(II) complexes of NHCs in acids catalyzed the formation of methyl esters with a high selectivity at 80 °C. The TON of the Pd catalyst could reach 41 when K₂S₂O₈ employed as the oxidant (Table 1.3).

Table 1.1 Modifications on Pt catalysts for homogeneous oxidation of methane to methyl bisulfate.

$\text{CH}_4 + \text{H}_2\text{SO}_4 \xrightarrow[\text{H}_2\text{SO}_4/\text{SO}_3]{\text{Pt catalyst}} \text{CH}_3\text{OSO}_3\text{H}$						
Entry	Catalyst	Temperature (°C)	Catalyst (mM)	Selectivity (%)	TOF (h ⁻¹)	TON
1 ^{b)}		220	50	81	36	Up to 500
2 ^{a)}		215	0.6	96	1 280	650
3 ^{a)}		215	3.3	>75	576	570
4 ^{a)}	(bipy)PtCl ₂	215	0.6	97	14 460	840
5 ^{a)}	(NH ₃) ₂ PtCl ₂	215	0.6	98	19 200	650
6 ^{a)}	PtCl ₂	215	0.6	97	15 300	770
7 ^{a)}	Pt(acac) ₂	215	0.68	97	22 500	880
8 ^{a)}	K ₂ PtCl ₄	215	0.6	98	Up to 25 000	Up to 16 000
9 ^{a)}	(DMSO) ₂ PtCl ₂	180	3	94	6 300	19 000

a) In 20% oleum.

b) In 98% H₂SO₄.

Bao and coworkers achieved a catalytic system for the direct aerobic oxidation of methane via the merging of Pd²⁺/Pd⁰, Q/H₂Q, and NO₂/NO in trifluoroacetic acid [31]. This method represents the first example utilizing an organic cocatalyst for the selective methane oxidation. The proposed catalytic cycle is described in Figure 1.4, Pd(II) is responsible for the C(sp³)-H insertion and leads to the formation of Pd(II)-methyl complex, which readily undergoes reductive elimination to form the oxidized product CF₃COOCH₃ and Pd(0) species. The single electron transfer between Pd(0) and benzoquinone (BQ) will regenerate Pd(II) for catalyst turnover. In order to achieve the catalytic cycle of BQ, NO₂ could functionalize as electron shuffle and can be generated with molecular oxygen serving as terminal oxidants.

Table 1.2 Homogeneous oxidation of methane to methyl bisulfate under strong acidic media.

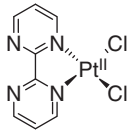
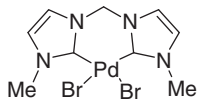
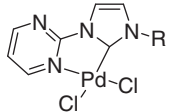
		CH ₄ $\xrightarrow[\text{Solvent, oxidant}]{\text{Metal catalyst}}$ CH ₃ OSO ₃ H					
Entry	Catalyst	Temperature (°C)	Solvent and oxidant	Conversion (%)	Selectivity (%)	TOF (h ⁻¹)	TON
1		220	102% H ₂ SO ₄	90	81	36	Up to 500
2	Hg(OSO ₃ H) ₂	180	100% H ₂ SO ₄	50	85	3.6	15
3	Au ⁰	180	3 M SeO ₃ in 96% D ₂ SO ₄	8	77	3.6	32
4	Au ⁰	180	3 M SeO ₃ in 96% D ₂ SO ₄ + 2% SO ₃	28	94	2.7	8
5	PdSO ₄	160	30% oleum	1	100	0.4	0.8

Table 1.3 Homogeneous oxidation of methane to methyl trifluoroacetate by Pd(II).

		CH ₄ + CF ₃ CO ₂ H $\xrightarrow[\text{CF}_3\text{CO}_2\text{H}]{\text{Pd(II), oxidant}}$ CF ₃ CO ₂ CH ₃			
Entry	Catalyst	Oxidant	Temperature (°C)	TON	
1	Pd(OCOC ₂ H ₅) ₂	H ₂ O ₂	90	5	
2		K ₂ S ₂ O ₈	90	30	
3	Pd(hfacac) ₂	H ₂ O ₂	50	50	
4	Pd(OAc) ₂ /Q/NO ₂	O ₂	80	7	
5		K ₂ S ₂ O ₈	80	41	
6 ^{a)}	PdCl ₂ (bpy)/Q/H ₃ PMo ₁₀ V ₂ O ₄₀	O ₂	80	118	

a) TFA/C₈F₁₈/H₂O was used.

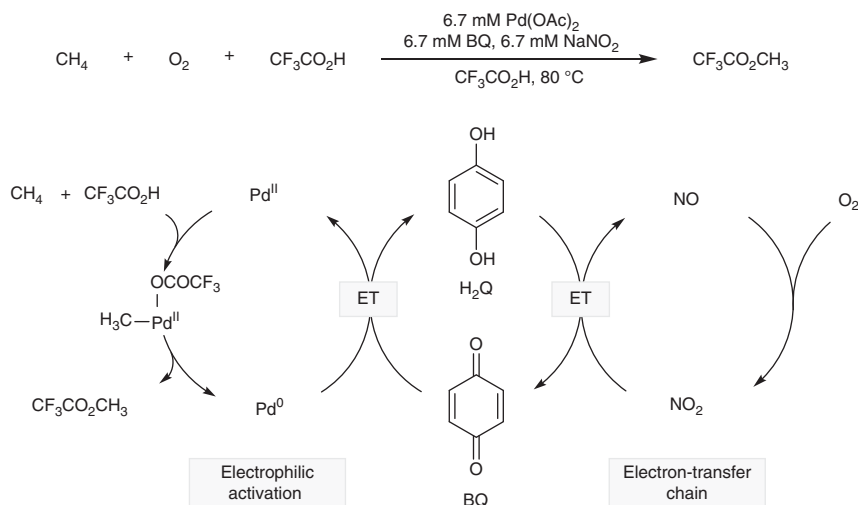


Figure 1.4 Combined redox couples for catalytic oxidation of methane by O_2 .

1.2.2 Radical-Mediated Activation

The activation of methane through a HAT process, albeit challenging due to the high $\text{C}(\text{sp}^3)\text{—H}$ BDE, has been demonstrated to be effective in producing the highly reactive methyl radical in situ within a homogenous system. Trapped by low-valency metal species or oxidized directly by oxygen, the methyl radical can thereby yield products containing methyl functionalized groups via either reductive elimination or direct oxidation, delivering methanol, formic acid, etc. as products.

Employing $\text{K}_2\text{S}_2\text{O}_8$ as the stoichiometric radical initiator, PdSO_4 as catalyst, fuming sulfuric acid as solvent, Sen and coworkers disclosed a highly chemoselective protocol for the direct C–H functionalization of methane, impressively methyl bisulfate was the only product [32]. A three-step, liquid-phase process initiated by urea– H_2O_2 system in combination with RhCl_3 catalyst was developed for the partial oxidation of methane to methanol, using SO_3 as the oxidant (Figure 1.5) [33]. In the first step, MSA is obtained through the capture of the methyl radical by SO_3 . Then, this intermediate was oxidized with a large excess of SO_3 at 160°C to furnish methyl bisulfate, which subsequently hydrolyzed to form the final product methanol.

In a relative weaker acidic trifluoroacetic acid media, selective methane C–H functionalization to methyl trifluoroacetate can be achieved by using a $\text{Cu(OAc)}_2/\text{K}_2\text{S}_2\text{O}_8$ catalyst system, with a TON of up to 151 and a nearly quantitative yield (96.3%) based

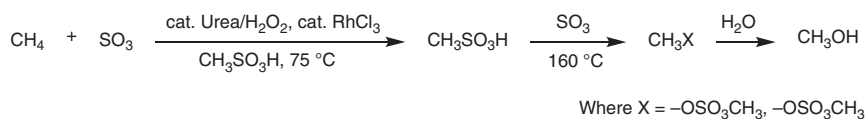


Figure 1.5 Radical-initiated oxidation of methane by $\text{K}_2\text{S}_2\text{O}_8$. Source: Modified from Mukhopadhyay et al. [33].

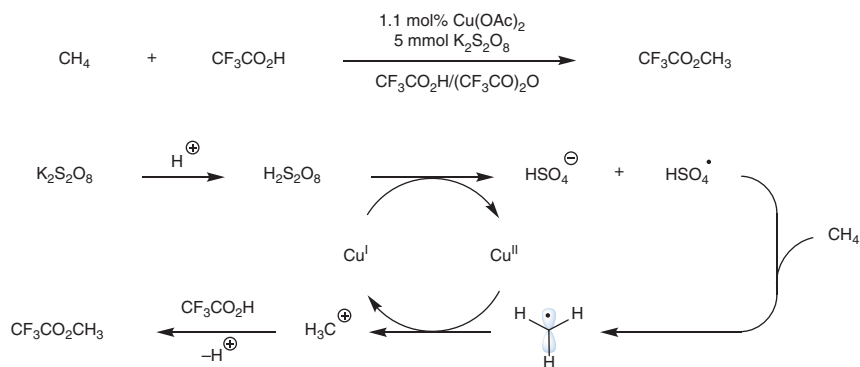


Figure 1.6 Cu(OAc)_2 -catalyzed methane oxidation. Source: Based on Yin et al. [34].

on the amount of methane (Figure 1.6) [34]. This copper catalyzed system is believed to be initiated by the single-electron oxidation of methyl radical into CH_3^\oplus species by the Cu(II) and then rapidly react with the solvent trifluoroacetic acid to obtain the methyl trifluoroacetate.

In 2018, van Bokhoven and coworker reported a selective method to convert methane to methyl trifluoroacetate at 90°C with low pressures (5 bar) using copper(II) oxide catalyst, resulting in a 63% yield with a TON of 33 and a 71% conversion [35]. Notably, a remarkable feature of the catalytic platform is the recyclability of the copper catalyst, which can be used a second time without significant decrease in the catalytic activity.

An elegant example of generating methyl radicals was reported by Periana lab, using a combination of chloride and iodate as oxidant [36]. The product methyl trifluoroacetate was obtained with good selectivity ($>85\%$) in 20% yield from methane. This metal-free process initiated by oxidative formation of chlorine radical, which was a competent HAT reagent to activate methane into highly reactive methyl radical. The resultant methyl radical was then trapped by I_2 to form methyl iodide, which can be subsequently converted into methyl trifluoroacetate in the trifluoroacetic acid solvent (Figure 1.7).

Hydroxyl radical was also proven to be an effective HAT agent to activate methane to generate methanol and methyl ester [37, 38]. Recently, the Ohkubo and Hirose developed a one-step process for the oxygenation of methane into methanol and formic acid using chlorine dioxide as an efficient radical precursor to generate chlorine radicals under light irradiation [39]. The key to the success of this process is the use of a perfluorinated solvent (i.e. perfluorohexane). By forming a two-phase system with water, good selectivity could be achieved that separated the products in the water phase from the oxidation process in the fluorous phase. In this way, 14% and 85% yields of methanol and formic acid, respectively, were obtained under ambient conditions, with a methane conversion of 99%, without the formation of further overoxidized products.

Recent, Hu and coworkers demonstrated that inexpensive FeCl_3 salt could catalyze the direct oxidation of methane with the employment of H_2O_2 as oxidant under

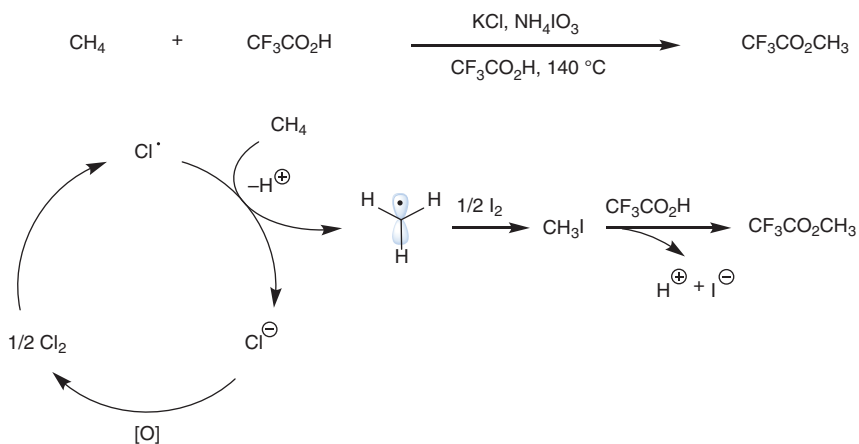


Figure 1.7 Functionalization of methane by iodate/chloride system.

a mild condition (50°C) in water [40]. Notably, the efficiency of this catalytic oxidation was evidenced by a remarkable yields of methanol ($1972.2 \mu\text{mol/gcat}$) and formic acid ($33\,273.5 \mu\text{mol/gcat}$), with a high TOF of 5.7h^{-1} .

Nature creates a unique radical-rebound mechanism to achieve highly selective methane aerobic oxidation, thusly form methanol selectively by methane monooxygenases (MMOs). Central to this strategy, a high-valent iron(IV) oxo cluster can easily abstract one hydrogen atom from methyl to release the methyl radical, which would be subsequently captured by the dinuclear iron cluster to generate methanol, avoiding the nonselective coupling of methyl radical with oxygen [41–43]. Although extensive mechanistic studies have been conducted, the challenges in efficient production of this active enzyme have hampered the use for industrial applications, driving the development of more robust catalytic system. In 2012, Arnold and coworkers reported a methane hydroxylation by cytochrome P450 using iodosylbenzene as the terminal oxidant [44]. Shortly after this report, Kamachi and coworkers described a modified photosynthetic system containing a particle methane monooxygenase (pMMO), where nicotinamide adenine dinucleotide (NADH) generated from water oxidation in the thylakoid was passed on to assistant the activation oxygen in the pMMO system [45]. In 2019, Lee and coworkers developed an innovative approach to produce pMMO-mimics in *Escherichia coli* through molecular reconstruction technologies [46]. In comparison to the native pMMO system, these easily accessible enzymes demonstrated comparable catalytic efficiency in methane oxidation.

1.3 Formation of Acetic Acid

Acetic acid is an important commodity feedstock widely used in the production of agrochemical, pharmaceutical, and polymer materials. The global demand for acetic acid is about 6.5Mt/a , of which approximately 5.0Mt/a is manufactured

from methanol. The industrial-scale production of acetic acid currently involves a three-step process based on the high-temperature conversion of methane to syngas, the conversion of syngas to methanol, and the carbonylation of the methanol to acetic acid. The direct carbonylation is implemented through the rhodium-catalyzed Monsanto process and the iridium-catalyzed Cativa process [47]. The intensive energy requirements, high cost, and multistep reaction required for this production process lead to its lower economy. In recent decades, significant research efforts have been made concerning the direct conversion of methane to acetic acid, of which direct C–H oxidative carbonylation represents an efficient route. Generally, oxidants are required in this cross coupling of methane and carbon monoxide, and often times play a significant role in the efficiency and selectivity. This section is organized based on the oxidants employed in the direct oxidative carbonylation of methane to acetic acid, including $K_2S_2O_8$, O_2 , H_2SO_4 , and other oxidants.

1.3.1 $K_2S_2O_8$ Oxidant-Based Systems

Because of its low toxicity, availability, and stability, $K_2S_2O_8$ has been found to be a suitable oxidant for oxidative reactions. In particular, it behaves not only as an oxidant but also as a source of initiated radicals during the direct conversion of methane to acetic acid. Through a $K_2S_2O_8$ -mediated reaction, Lin and Sen achieved the first example of oxidative carbonylation of methane with CO in water (Table 1.4) [48]. A mode of hydrogen-atom abstraction process by the sulfate radical species, generated from $K_2S_2O_8$, for methane oxidative conversion to acetic acid was proposed in this approach. In the same year, Fujiwara et al. reported the first catalytic approach of $Pd(OCOEt)_2/CuSO_4$ -catalyzed direct carbonylation of methane to acetic acid mediated by $K_2S_2O_8$ oxidant [49]. This reaction can be catalyzed by $Pd(OCOEt)_2$ and $CuSO_4$ individually or in combination, but the highest yield was obtained when $CuSO_4$ was used as the catalyst alone. In the following decade, the search for an efficient catalyst for the synthesis of acetic acid from methane employing $K_2S_2O_8$ as the oxidant was continued by the Fujiwara group, namely, a $Cu(OAc)_2$ catalyst [50], a Yb_2O_3 catalyst [51], a $VO(acac)_2$ catalyst [52, 53], a Mg catalyst [54], a $Co(OAc)_2$ catalyst [55, 56], a $CaCl_2$ catalyst [57], and a Mo/ $CaCl_2$ catalyst [58]. Among them, the $VO(acac)_2$ catalyst demonstrated the highest conversion efficiency, achieving 97% and 93% molar yields of acetic acid based on methane using CO_2 [52] and CO [53] as the carbonylating agents, respectively. In addition, $CaCl_2$ is also an effective catalyst, providing a 93.8% molar yield from methane after 140 hours.

Bell and coworkers also studied the direct transformation of methane and CO_2 to acetic acid using a $VO(acac)_2$ and $K_2S_2O_8$ catalytic system [59]. They found that the acetic acid is predominantly formed by the reaction of methane and trifluoroacetic acid with the coproduction of CHF_3 when the solvent is trifluoroacetic acid. Note that the reaction of methane with CO_2 is thermodynamically unfavorable; however, the transformation of methane with trifluoroacetic acid is thermodynamically favorable [60, 61]. In this protocol, an ~7% conversion of methane to acetic acid was

Table 1.4 Direct conversion of methane to acetic acid utilizing $K_2S_2O_8$ as the oxidant.

$\text{CH}_4 + [\text{CO}] \xrightarrow[\text{K}_2\text{S}_2\text{O}_8, \text{ solvent}]{\text{Catalyst}} \text{CH}_3\text{CO}_2\text{H}$							
Entry	Catalyst	[CO] ^{a)}	Solvent	Temperature (°C)	TON ^{b)}	TOF (h ⁻¹) ^{c)}	Yield ^{d)} (%)
1	None	CO	D ₂ O	105–115	—	—	n.a.
2	CuSO ₄	CO	CF ₃ CO ₂ H	80	39.4	0.88	1
3	Cu(OAc) ₂	CO	CF ₃ CO ₂ H	80	111.3	5.57	0.9
4	Yb ₂ O ₃	CO	CF ₃ CO ₂ H	80	1	0.05	n.a.
5	VO(acac) ₂	CO ₂	CF ₃ CO ₂ H	80	24	1.20	97
6	Mg	CO	CF ₃ CO ₂ H	80	0.05	0.002	1
7	Co(OAc) ₂	CO	CF ₃ CO ₂ H	70	0.2	0.02	0.1
8	VO(acac) ₂	CO	CF ₃ CO ₂ H	80	30	1.5	93
9	CaCl ₂	CO	CF ₃ CO ₂ H	80	30.5	0.15	93.8
10	Mo/CaCl ₂	CO	CF ₃ CO ₂ H	85	17	0.85	89.4
11	VO(acac) ₂	CO ₂	Fuming H ₂ SO ₄	85	n.a.	n.a.	7
12	Ca[V(ON(CH(CH ₃)CO ₂) ₂) ₂]	None	CF ₃ CO ₂ H	80	13.4	0.67	29.4
13	HPA	CO	CF ₃ CO ₂ H	80	3000	150	20
14	Ca[V(HIDA) ₂]	CO	CF ₃ CO ₂ H	80	5630	281.5	54

a) Carbonylating agent.

b) Turnover number (moles of acetic acid per mole of catalyst).

c) Turnover frequency (moles of acetic acid per mole of catalyst per hour).

d) Highest molar yield (%) of acetic acid based on methane.

n.a., not applied.

obtained when fuming sulfuric acid was utilized as the solvent, and the formation of $\text{CH}_3\text{SO}_3\text{H}$ was inhibited in the presence of CO_2 under these reaction conditions. Specially, the water formed during this process must be absorbed in an accompanying reaction for the overall thermodynamics to be favorable.

The Pombeiro group achieved the direct conversion of methane into acetic acid employing vanadium complexes with N, O-, O, O-ligands, or heteropolyacids as catalysts and $\text{K}_2\text{S}_2\text{O}_8$ as the oxidant [62–64]. In these reactions, the highest molar yield of acetic acid from methane was 54%, and the TON was up to 5630. The catalyst still remained active after its solution was recycled multiple times, and the recycling of the reaction procedure was conducted by simply added new portions of the $\text{K}_2\text{S}_2\text{O}_8$ oxidant and the methane and CO for each run. Density functional theory mechanistic studies have shown that this carboxylation of methane proceeds through a radical mechanism, involving the sequential formation of methyl radicals, acetyl radicals, and peroxyacetyl radicals. Upon hydrogen atom abstraction from the trifluoroacetic acid or the methane, this process yields acetic acid (Figure 1.8).

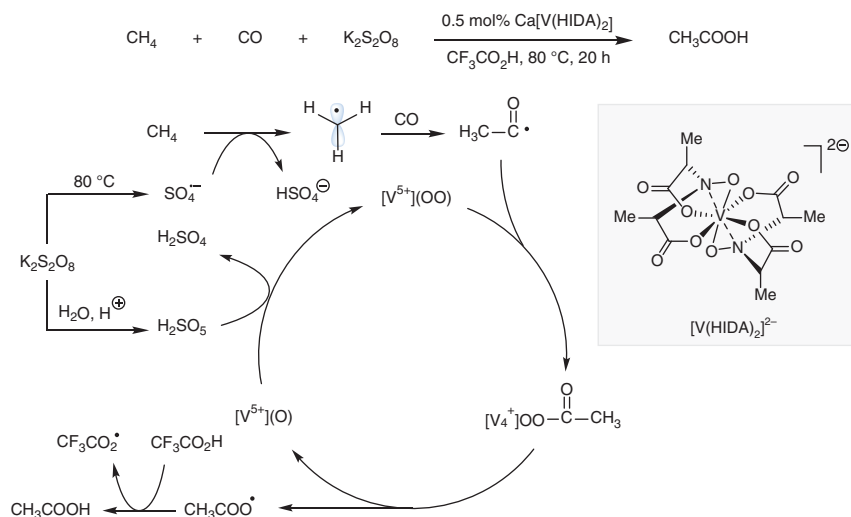


Figure 1.8 Proposed mechanism of the radical formation and carboxylation of methane to acetic acid.

1.3.2 O₂ Oxidant-Based Systems

O₂, which constitutes 20.95% of the Earth's atmosphere, is one of the most abundant, inexpensive feedstock materials. From a commercial point of view, direct catalytic transformation of methane into acetic acid employing O₂ as the oxidant would be an ideal process. Nevertheless, the thermodynamic driving force of the C–O band formation between methane and oxygen, compared to the sluggish coupling of methane and carbon monoxide, has resulted in a significant challenge to achieve selective formation of acetic acid in the presence of C1 oxidative products. The first to demonstrate the feasibility of catalytic oxidative carbonylation of methane to acetic acid under O₂ oxidant conditions were Lin and Sen [65], using the RhCl₃–HCl–HI (KI) catalytic system in an aqueous medium, and Fujiwara et al. [66], employing Pd(OAc)₂/Cu(OAc)₂ as the catalyst in trifluoroacetic acid (Table 1.5). The TOF of the acetic acid was 0.07 h⁻¹ under reaction conditions developed by the Sen et al. and 0.10 h⁻¹ under reaction conditions developed by Fujiwara et al. In addition, Sen et al. showed that MeOH was not transformed into acetic acid under their reaction conditions but was oxidized to formic acid. The role of I⁻ in this protocol has not yet been unambiguously determined. In addition, CO can be replaced with CO₂ in the Fujiwara et al. system, resulting in a TOF of 0.83 h⁻¹. Further studies based on the RhCl₃–Cl⁻–I⁻ catalytic system were conducted by Sen and coworkers [67], Grigoryan and coworkers [68], and Chepaikin et al. [69], and they used C₃H₇CO₂H/D₂O, CD₃CO₂D/D₂O, and CF₃CO₂D/D₂O aqueous mediums, respectively. In these processes, improved yields were obtained for the oxidative carbonylation of methane. Shul'pin and coworkers achieved the vanadium complex-catalyzed carboxylation of methane with CO or CO₂ in an aqueous solution [70]. The TON of the acetic acid was 37 after 50 hours at 100 °C

Table 1.5 Direct transformation of methane to acetic acid using O₂ as the oxidant.

$\text{CH}_4 + [\text{CO}] \xrightarrow[\text{O}_2, \text{ solvent}]{\text{Catalyst}} \text{CH}_3\text{CO}_2\text{H}$						
Entry	Catalyst	[CO] ^{a)}	Solvent	Temperature (°C)	TON ^{b)}	TOF (h ⁻¹) ^{c)}
1	RhCl ₃	CO	D ₂ O	95	27.6	0.07
2	RhCl ₃ · 3H ₂ O	CO	C ₃ H ₇ CO ₂ H/ HFIP/D ₂ O	80	44	1.29
3	RhCl ₃	CO	CD ₃ CO ₂ D/ D ₂ O	95	10	0.42
4	RhCl ₃ · 4H ₂ O	CO	CF ₃ CO ₂ D/ D ₂ O	95	n.a.	n.a.
5	Pd(OAc) ₂ / Cu(OAc) ₂	CO	CF ₃ CO ₂ H	80	4.1	0.1
	Pd(OAc) ₂ / Cu(OAc) ₂	CO ₂ ^{d)}	CF ₃ CO ₂ H	80	16.5	0.83
6	NaVO ₃	CO	H ₂ O	100	37	0.74
	NaVO ₃ /PCA	CO ₂ ^{e)}	H ₂ O	40	20	0.67
7	K ₂ PdCl ₄ / H ₅ PMo ₁₀ V ₂ O ₄₀	None	CF ₃ CO ₂ H	80	4167	520.85

a) Carbonylating agent.

b) Turnover number (moles of acetic acid per mole of catalyst).

c) Turnover frequency (moles of acetic acid per mole of catalyst per hour).

d) K₂S₂O₈ was used as the oxidant.

e) H₂O₂ was used as the oxidant.

n.a., not applied.

in the presence of O₂ and an NaVO₃ catalyst. Likewise, when the reaction was conducted in an NaVO₃ and pyrazine-2-carboxylic acid (PCA) catalyst system with H₂O₂ as the oxidant, the TON of the acetic acid was 22 after 50 hours at 40 °C. In addition, CO₂ can be used instead of CO in this approach, resulting in a TON of 20 for the acetic acid after 30 hours at 40 °C. Recently, Hao et al. reported the K₂PdCl₄ and H₅PMo₁₀V₂O₄₀ (HPA)-catalyzed partial oxidation of methane using O₂ as the oxidant at a low temperature [71]. The TON of acetic acid was as high as 4167, and the conversion of methane was up to 11% after eight hours at 80 °C.

1.3.3 H₂SO₄ Oxidant-Based Systems

Transition metal-catalyzed oxidative conversions of methane to acetic acid in liquid sulfuric acid have been established, wherein H₂SO₄ not only serves as a reaction solvent but also as an oxidant. Periana et al. achieved the Pd-catalyzed, highly selective oxidative condensation of two methane molecules to acetic acid in one step (Figure 1.9) [72, 73]. The proposed electrophilic C—H bond activation of methane by

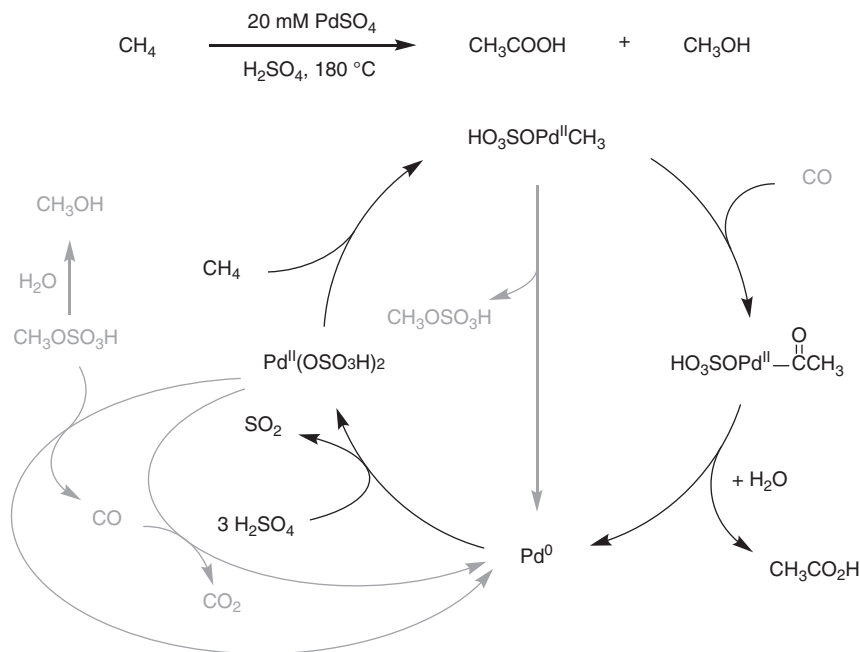


Figure 1.9 Proposed mechanism for the oxidative condensation of two methane molecules to acetic acid.

the Pd(II) species to generate a Pd-CH₃ intermediate is crucial to this reaction. The methyl group of the acetic acid originates from the methane, and the carboxyl group originates from the MeOH, which is also generated in situ from the methane. The product selectivity of this reaction is reported to be as high as 90%, while the catalytic efficiency remains low. Although MeOH is the precursor of CO, the addition of high concentrations of CO causes the reaction to shut down because the reduction rate of Pd(II) with CO outstrips the reoxidation rate of Pd(0). As a result, the carbonylation process occurs only at low levels of CO via the in situ oxidation of methanol. This tandem catalysis involves methane electrophilic C-H bond activation to generate Pd-CH₃ species, followed by the efficient oxidative carbonylation with MeOH generated in situ from methane to form acetic acid. In this transformation, concentrated H₂SO₄ is the oxidant used for the reoxidation of the Pd(0) species to Pd(II) intermediates in the catalytic cycle, and this process is believed to be the rate-determining step. This step can be accelerated dramatically; however, when CuCl₂ and O₂ are introduced to the reaction mixture [74]. Consequently, the yield of acetic acid is increased significantly compared with that obtained utilizing PdSO₄ alone. Bell et al. investigated the effects of the reaction conditions and mechanism in detail, including identifying CO as a reaction intermediate and identifying an intermolecular process in the generation of the products [75].

In addition to the Pd-catalyzed oxidative conversion of methane to acetic acid in liquid sulfuric acid, the Pt(II) catalyst can be used as an alternative catalyst for this reaction. Zerella and Bell described the Pt-catalyzed oxidative carbonylation of

methane to acetic acid in fuming or concentrated sulfuric acid [76]. In this approach, the H_2SO_4 oxidizes the Pt(II)-CH_3 species generated from the methane electrophilic C—H bond activation with monomeric PtX_2 to Pt(IV)-CH_3 . The overall production of liquid-phase products is greater when fuming H_2SO_4 is used, but the selectivity of acetic acid formation is greater when concentrated H_2SO_4 is used. Adding neutral ligands such as bpy or bpym to Pt(II) could not affect the activity or the production of acetic acid. Moreover, when CuCl_2 and O_2 are employed in this reaction, the catalyst activity can be increased by promoting the reoxidation process. Specifically, excessively high CO partial pressures should be avoided when using this method because it reduces the active Pt(II) to inactive Pt(0) . Thus, to minimize or avoid the loss of the active Pt(II) species, a balance between oxidizing and reducing conditions must be maintained during the reaction. This approach provides a method for the direct carbonylation of methane to acetic acid; however, the selectivity to acetic acid needs to be improved further.

1.3.4 Other Oxidant-Based Systems

Alternative methods for the carbonylation of methane with CO include the use of SbF_5 and NaClO as oxidants. Hogeveen et al. [77], Olah and coworkers [78], and Horváth and coworkers [79] independently achieved the selective formation of acetic acid from methane in liquid superacids (i.e. HF/SbF_5 or $\text{HSO}_3\text{F/SbF}_5$). SbF_5 oxidizes methane into methyl cations $[\text{CH}_3]^+$ instead of $[\text{CH}_5]^+$ with the concomitant stoichiometric generation of SbF_3 . The exclusive formation of acylium ion ($[\text{CH}_3\text{CO}]^+[\text{SbF}_6]^-$) and acetic acid through an aqueous work-up can be obtained through the electrophilic activation of methane with CO and superacids. The selectivity of this approach is achieved by the full protection of the initial product, that is, the acylium ion ($[\text{CH}_3\text{CO}]^+[\text{SbF}_6]^-$), which does not react with methane, CO, or the extremely strong electrophilic HF/SbF_5 . Fujiwara et al. reported on the lanthanide-catalyzed direct carboxylation of methane to acetic acid with CO in water, with NaClO as the oxidant (Figure 1.10) [80]. Yb(III) acetate $[\text{Yb(OAc)}_3]$ has the best catalytic activity among the lanthanide catalysts, and the best result was achieved with a promoter at an Mn(OAc)_2 -to- Yb(OAc)_3 ratio of 1 : 10. A highest yield (2.8% based on methane) and TON (69) were obtained using this catalyst system. Mechanistically, upon being reduced by Mn^{2+} , Yb^{3+} is converted into Yb^{2+} , which is oxidized by NaClO to form an oxo Yb radical ($\text{Yb}^{3+}\text{-O}\cdot$). The oxo radical abstracts a hydrogen atom from the methane to produce a methyl radical, which reacts with CO to produce an acetyl radical. Then, the acetyl radical is converted to an acetyl cation by Mn^{3+} . Finally, the acetyl cation reacts with water to produce acetic acid.

1.4 Formation of Methanesulfonic Acid

MSA is a strong organic acid that is widely used in the pharmaceutical and electroplating industries and in energy storage and metal recycling [81]. The current

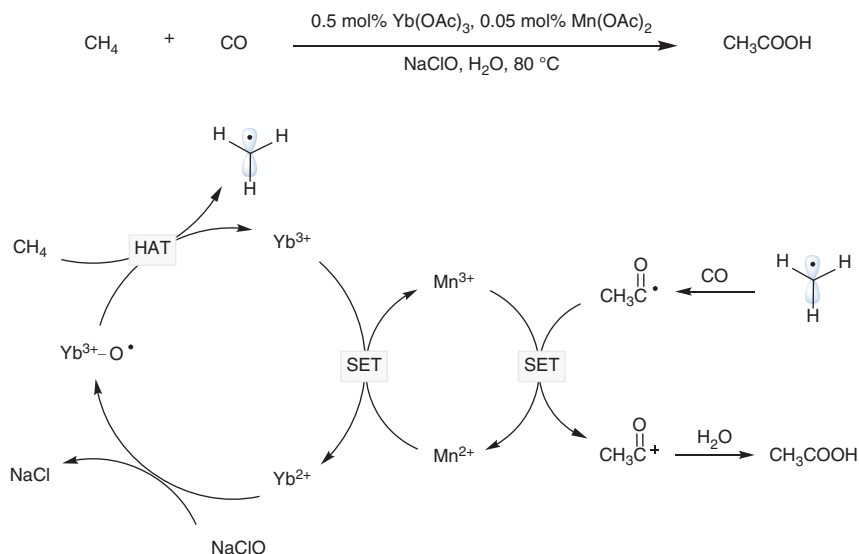


Figure 1.10 Yb(OAc)_3 -catalyzed carboxylation of methane to acetic acid. Source: Modified from Asadullah et al. [80].

process for the synthesis of MSA involves chlorine oxidation of methylmercaptan [82]. In this process, 6 mol of HCl are produced per mole of MSA. The formation of a large amount of by-product remains one potential problem with this method. In recent years, the direct sulfonation of methane to MSA, which avoids the coproduction of HCl , has received considerable attention because of the abundance of raw materials available for this process. Early studies by Sen et al. and Bell et al. have shown that SO_3 can be employed as a sulfonating reagent in fuming sulfuric acid in the presence of various initiators (or catalysts), such as $\text{K}_2\text{S}_2\text{O}_8$ [32, 82], urea- H_2O_2 [83], CaO_2 [84], $\text{K}_4\text{P}_2\text{O}_8$ [85], $\text{Hg}(\text{CF}_3\text{SO}_3)_2$ [86], and $\text{Ce}(\text{SO}_4)_2$ [87] (Table 1.6). Later, Bell and coworkers and Shaabani and Ghadari also accomplished such transformations using SO_2 [88, 89] or chlorosulfonic acid (CSA) [90] as sulfonating reagents instead of SO_3 . These sulfonated protocols are initiated by the thermal decomposition of the initiators, which generates the radical anions. However, these procedures suffer from several disadvantages, such as expensive metal catalysts, low yields, and conversions, which make them unsuitable for large-scale production.

Critically, the exploitation of an industrial chemical process for the direct sulfonation of methane to MSA with high atomic economy, scalability, and high selectivity holds great importance. Recently, Díaz-Urrutia and Ott reported a selective sulfonation protocol for the production of MSA with high levels of selectivity and efficiency (Figure 1.11) [91]. In this reaction, methane and SO_3 are the only two reactants, and the electrophilic initiators monomethylsulfonylperoxide sulfuric acid (MMSP) or dimethyl sulfoniopropionate (DMSP) can be prepared in situ. In particular, this process is readily scalable with a production of up to 20 metric tons per year of MSA. On the basis of extensive studies and mechanistic investigations, an ionic reaction mechanism has been proposed for this method instead of a radical mechanism. Initially,

Table 1.6 Direct sulfonation of methane to MSA by various initiators initiated.

		CH ₄ + [SO]		Initiator Solvent		CH ₃ CO ₂ H			
Entry	Initiator	[SO] ^{a)}	Solvent	Temperature (°C)	TON ^{b)}	TOF (h ⁻¹) ^{c)}	Selectivity (%)	Yield ^{d)} (%)	
1	K ₂ S ₂ O ₈	SO ₃	Fuming H ₂ SO ₄	90	—	—	n.a.	35	
2	K ₂ S ₂ O ₈	SO ₃	Fuming H ₂ SO ₄	60	—	—	n.a.	80	
3	Urea/H ₂ O ₂	SO ₃	Fuming H ₂ SO ₄	65	—	—	99.9	86	
4	CaO ₂	SO ₃	Fuming H ₂ SO ₄	65	—	—	n.a.	91	
5	K ₄ P ₂ O ₈	SO ₃	Fuming H ₂ SO ₄	95	—	—	n.a.	26	
6	Hg(CF ₃ SO ₃) ₂ (cat.)	SO ₃	Fuming H ₂ SO ₄	148	123.2	24.64	87	44	
7	Ce(SO ₄) ₂ (cat.)	SO ₃	Fuming H ₂ SO ₄	130	54	1.29	99.9	23	
8	K ₂ S ₂ O ₈	SO ₂	CF ₃ SO ₃ H	65	—	—	n.a.	22	
9	PdCl ₂ /CuCl ₂ (cat.)	SO ₂	CF ₃ SO ₃ H	85	11.8	0.3	n.a.	20	
10	Ce(SO ₄) ₂ (cat.)	CSA	CSA	130	22.4	0.93	n.a.	15	

a) Sulfating agent.

b) Turnover number (moles of MSA per mole of catalyst).

c) Turnover frequency (moles of MSA per mole of catalyst per hour).

d) Molar yield (%) of MSA based on initial amount of SO₃ (SO₂ or CSA).

n.a., not applied.

the electrophilic initiator (MMSP or DMSP) can be protonated into a peroxonium ion under superacidic conditions, resulting in a superelectrophilic oxygen atom that can trigger the sulfonation of methane. Finally, the electrophilic initiator decomposes to MSA or H₂SO₄.

1.5 Formation of Borylated Products

The direct borylation of methane via C–H activation is a highly effective strategy for converting abundant methane to organoboron chemicals, which can be used as important synthetic building blocks for the construction of complex molecules in transition metal catalyzed coupling reactions, such as Suzuki–Miyaura coupling [92]. Recently, Sanford and coworkers and Mindiola

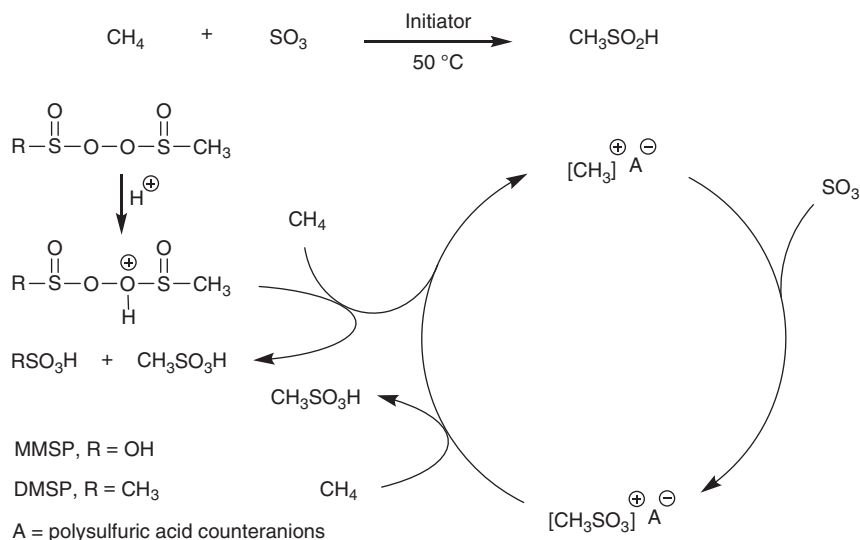


Figure 1.11 Electrophilic initiator triggered direct sulfonation of methane. Source: Díaz-Urrutia and Ott [91].

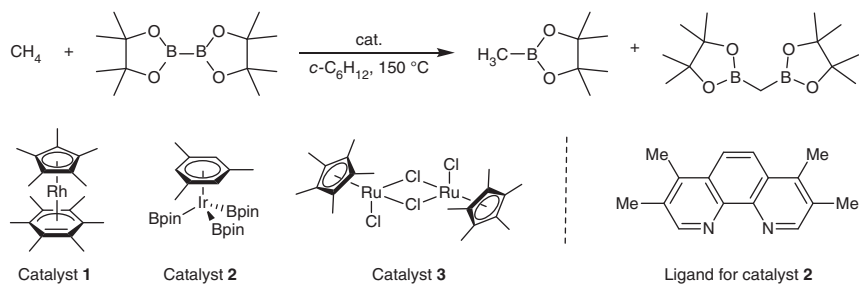


Figure 1.12 Catalyst-controlled selectivity in the C–H borylation of methane. Source: Modified from Cook et al. [93].

coworkers independently reported on transition metal-catalyzed C–H borylation of methane with bis-pinacolborane (B_2pin_2) in a cyclohexane solvent [93, 94]. Sanford and coworkers used iridium, rhodium, and ruthenium complexes as the catalysts, and the highest TON (68) was obtained for a 0.75 mol% loading of catalyst **1** (Figure 1.12) [93]. In this transformation, cyclohexane proved to be the optimal solvent, with only traces ($\sim 2\%$) of the solvent C–H borylation product. Specifically, different catalysts structure resulted in obvious differences in the reaction rates and selectivities. Catalyst **1** was approximately four times faster than catalyst **2** and catalyst **3**, but catalyst **3** had an initiation period of about two hours. The monoborylated-to-diborylated methane ratio was 4 : 1 when catalyst **2** was used. Switching to catalyst **1** and catalyst **3**, the ratio increased to 9 : 1 and 21 : 1, respectively.

On the basis of a combination of high-throughput screening and computational mechanism discovery techniques, Mindiola et al. identified an improved phosphine

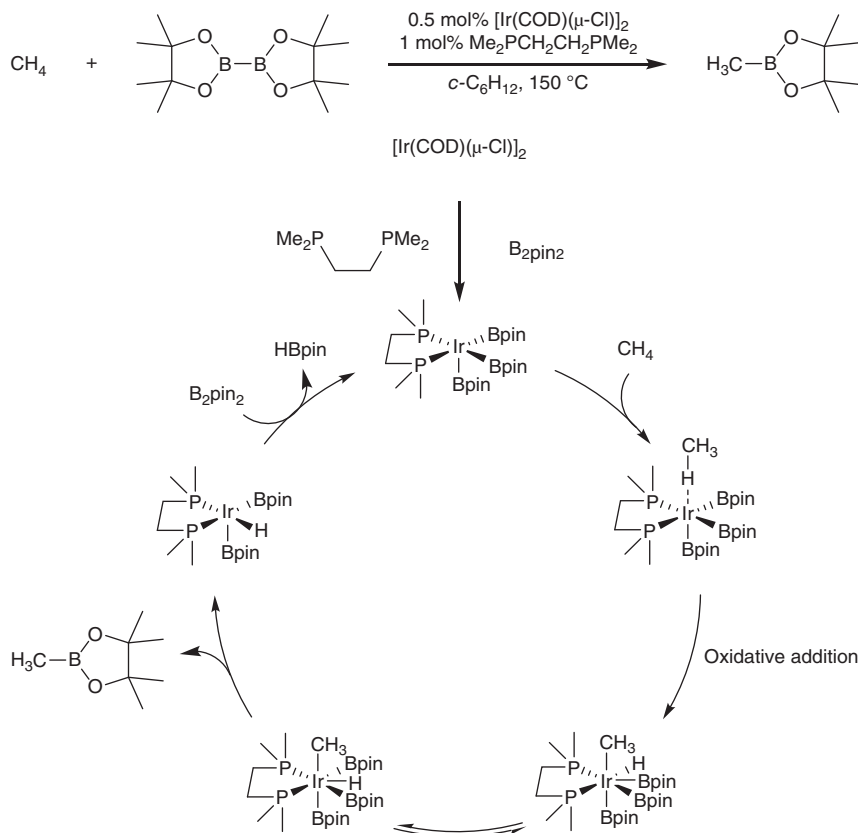


Figure 1.13 Iridium-catalyzed borylation of methane [95].

ligand, which led to yield up to 52% and TONs of up to 104 and improved the selectivity for mono- vs. diborylated methane has been obtained [94]. Further investigations revealed that the use of the soft Lewis base ligand lowered the activation barrier of the rate-determining step, and a maximum TON of 170 with a selectivity of 9 : 1 for monoborylated to diborylated methane could be achieved [95]. In the proposed catalytic cycle (Figure 1.13), the dinuclear precursor undergoes ligand exchange to form a mononuclear catalyst, which reacts with B_2pin_2 at high temperatures to form the active state of the catalyst. Then, the active catalyst undergoes the oxidative addition of methane, followed by reductive elimination to produce the target product CH_3Bpin . Finally, the oxidative addition of B_2pin_2 with the Ir(III) species followed by a second reductive elimination step closes the cycle along with the formation of HBpin .

1.6 Formation of Aminated Products

Aliphatic amines are one of the most important building blocks in organic synthesis. The groups attached to the nitrogen atom are responsible for regulating the physical

properties and for controlling the key biological interactions. Consequently, aliphatic amines are ubiquitous in a large number of natural products, advanced materials, and pharmaceuticals [96]. The direct conversion of methane to aminated products by C—H bond activation would upgrade methane from an abundant feedstock to a value-added liquid commodity chemical, which is beneficial to reduce transportation costs and emissions. Recently, Zuo and coworkers reported a photocatalytic HAT strategy for the selective C—H amination of methane at ambient temperatures by using inexpensive cerium catalyst (Figure 1.14) [97]. In this work, the alkoxy radical serves as competent HAT reagent (O—H BDE \approx 105 kcal/mol) to activate the inert C—H bond of methane (C—H BDE \approx 105 kcal/mol), which can be regenerated efficiently from corresponding alcohols via ligand-to-metal charge transfer (LMCT) under visible-light irradiation. Notably, the polarity matching effect of the alkoxy radical-mediated HAT has suppressed the HAT event with the solvent, thusly the oxidation of solvent has been inhibited, providing a high level of selectivity for the desired product. In one of the optimized conditions, using ditertbutyl azodicarboxylate (DBAD) as cross-coupling reagent, in the presence of 20 mol% 2,2,2-trichloroethanol (TCE) and 0.01 mol% $\text{Ce}(\text{OTf})_4$, methane can be converted to liquid product Boc-protected methyl hydrazine in 29% yield with a high catalyst TON of 2900. Slightly modifying the conditions from 0.01 mol% $\text{Ce}(\text{OTf})_4$ to 0.5 mol% $(\text{Bu}_4\text{N})_2\text{CeCl}_6$ could improve the yield to 63%. Apart from the amination of methane, alkylation and arylation of methane could also be facily achieved by this alkoxy radical-mediated HAT strategy with the employment of electron-deficient alkenes and heteroarenes as radical trapping reagents. Moreover, through the application of continuous flow technology for mixed-phase gas/solution reactions, this photocatalytic transformation could be scaled up using a micro flow reactor. In

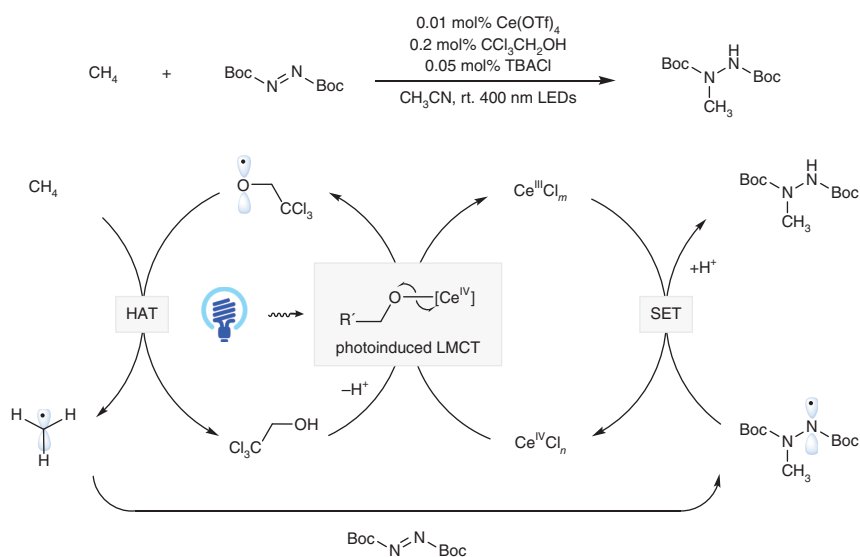


Figure 1.14 Cerium-catalyzed amination of methane under ambient temperature.

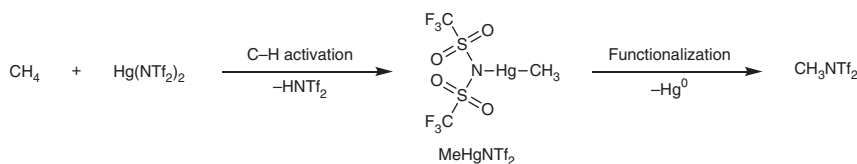


Figure 1.15 Selective transformation of methane to aminated products by Tl(III) and Hg(II)-directed C–H activation.

the proposed catalytic cycle, the alcohol could coordinate with cerium salts to form Ce(IV) alkoxy complex, which could undergo a LMCT-homolysis event to cleave the Ce–O bond into a high-energy electrophilic alkoxy radical and a reduced Ce(III) species. The alkoxy radical then abstracts a hydrogen atom from methane to generate a methyl radical species, which readily couple with the DBAD to form a new C–N bond. The desired product is formed after a single-electron reduction with the Ce(III) species, and the cerium catalytic cycle is then completed.

In addition to the photoinduced alkoxy radical-mediated HAT activation mode, electrophilic C–H activation followed by the metal-alkyl functionalization reaction strategy has been demonstrated as an effective approach to the direct amination of methane. Periana et al. achieved the selective transformation of methane using highly electrophilic, main-group oxidants based on Tl(III) and Hg(II) directed C–H activation (Figure 1.15) [98]. The methane-aminated product MeNTf_2 was generated with a selectivity of 92% and a yield of 50% based on added $\text{Tl}^{\text{III}}(\text{TFA})_3$; however, a lower yield of ~5% was obtained when $\text{Hg}^{\text{II}}(\text{NTf}_2)_2$ was used.

1.7 Formation of Alkylated Products

Employing methane as a C1 feedstock for alkylated reactions is as an ideal approach to sustainable synthesis because of its atom economy and the abundance of raw materials available. Typically, harsh reaction conditions are required to enable C–H bond cleavage of methane, rendering them inexpedient for broad applications. In this context, a selective and direct methane functionalization under mild reaction conditions would be more practical. Pérez coworkers established a silver-catalyzed C–C bond formation between methane and ethyl diazoacetate (EDA) in supercritical CO_2 (scCO_2) (Figure 1.16) [99]. This reaction employs scCO_2 as the reaction medium, which is inert with respect to the reactive intermediates and completely miscible with methane, has a strong solvating ability toward EDA, making it the key to the success of this reaction. This protocol utilizes a silver catalyst bearing perfluorinated indazolylborate ligands, which helps increase the solubility of the silver catalyst in scCO_2 , resulting in a 19% yield of the methane-alkylated product, with TONs of up to 478 under optimized conditions. A mechanism for the alkylation of methane, including silver-catalyzed N_2 elimination from the EDA and carbene transfer mediated by a highly electrophilic silver carbene intermediate, also has been proposed.

Further investigation has revealed that catalyst **5** is the most active of the series, with a TON of 734 and a TOF of 50.4 h^{-1} [100]. Moreover, reducing the equivalent

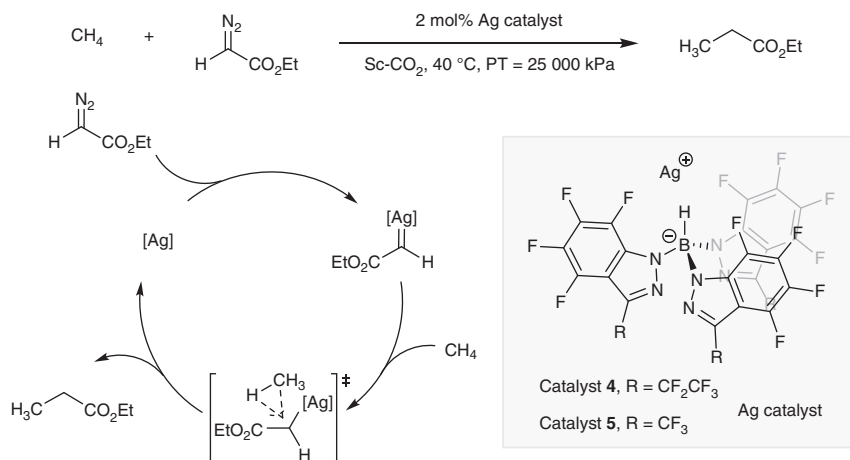


Figure 1.16 Silver-catalyzed C–C bond formation between methane and ethyl diazoacetate in scCO_2 .

of the catalyst, controlling the partial pressure ratio of the CO_2 , and maintaining a lower concentration of EDA substrate can effectively inhibit side reactions, such as the coupling of EDA. In addition, researchers found that the carbene species formed by the copper-based catalyst can also produce alkylation of methane with scCO_2 as the reaction solvent [101]. Although the yield is only 4%, it paves the way for the development of a more economical catalytic system.

In addition to the advancement of transition metal catalysis, photocatalyzed C–H bond functionalization emerges as another promising approach for selective alkylation. The Noël group reported a mild alkylation protocol for methane alkylation using inexpensive decatungstate as the photocatalyst in the continuous flow reactors (Figure 1.17) [102]. Under the irradiation of UV light, with 5 mol% decatungstate catalyst, alkylation products of methane with various electron-deficient alkenes can be obtained with 38–48% yields. Notably, d_3 -acetonitrile is used as the solvent in this method to suppress alkylation product derived from CH_3CN activation. In the proposed mechanism, upon photoexcitation, HAT event between methane and excited tetrabutylammonium decatungstate (TBADT) would generate nucleophilic methyl radicals, which can be readily trapped by electron-deficient alkenes to form a new C–C bond and a carbon-centered radical. A subsequent HAT with the resultant radical intermediate would deliver the desired product and furnish the catalytic cycle.

1.8 Summary and Conclusions

Within 40 years, significant progress has been made in the direct conversion of methane, demonstrating intriguing opportunities to synthesize value-added products from this abundant C1 feedstock. A series of direct C–H functionalizations, such as hydroxylation, carbonylation, sulfonylation, alkylation, boronization, and amination, have been achieved. The direct conversion of methane into a variety

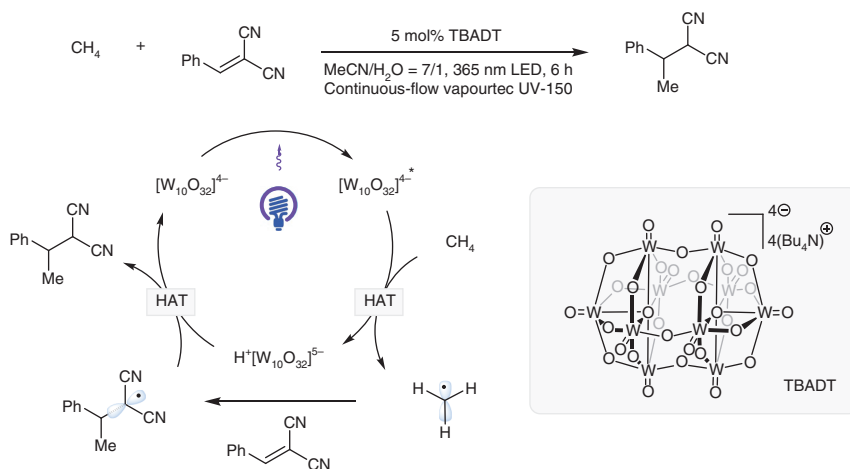


Figure 1.17 Decatungstate photocatalyst in flow enables the alkylation of methane.

of value-added liquid chemicals, such as methanol derivatives, acetic acid, and MSA, has demonstrated the vast synthetic potential of this C1 feedstock material. Although the catalytic efficiency and the cost-effectiveness of the employed catalysts and reagents are far from meeting the requirements for industrial applications, these groundbreaking developments have demonstrated that reactive intermediates, including methyl cation, methyl radical, and methyl metal complexes, can be generated and utilized under mild homogenous conditions for the effective C–H functionalizations of methane. Nevertheless, the tuning of these highly reactive intermediates to achieve a high selectivity and practical transformations will continue to drive the development of innovative catalytic strategies.

Transition metal catalysis has been demonstrated as a powerful platform to enable diverse applications in this field. Through the enabling $\text{C}(\text{sp}^3)\text{--H}$ insertion, methane can be selectively activated and coupled with various coupling reagents. Nevertheless, more transformations remain to be developed. For example, the oxidative oligomerization of methane remains a long-standing challenge. In a recent stoichiometric study, Sanford et al. demonstrated that ethane can be generated from the reductive elimination of a Pd(IV) intermediate (Figure 1.18) [103]. The exploitation of this strategy in combination with C–H insertion could possibly lead to a catalytic oxidative oligomerization of methane.

Innovative catalytic modes, including photoredox catalysis and electrocatalysis, recently have been introduced in organic synthesis, enabling a variety of selective transformations under otherwise unattainable conditions. Photoredox catalysis [104], which uses visible light energy for chemical activation, has drawn considerable research attention in the past decade [105, 106]. This powerful catalytic mode can produce highly reactive open-shell intermediates under ambient temperature, greatly facilitating the ability to overcome the high activation barrier without the need for high-temperature conditions. As has been demonstrated in recent seminal studies, diverse C–H functionalizations of methane have been implemented under

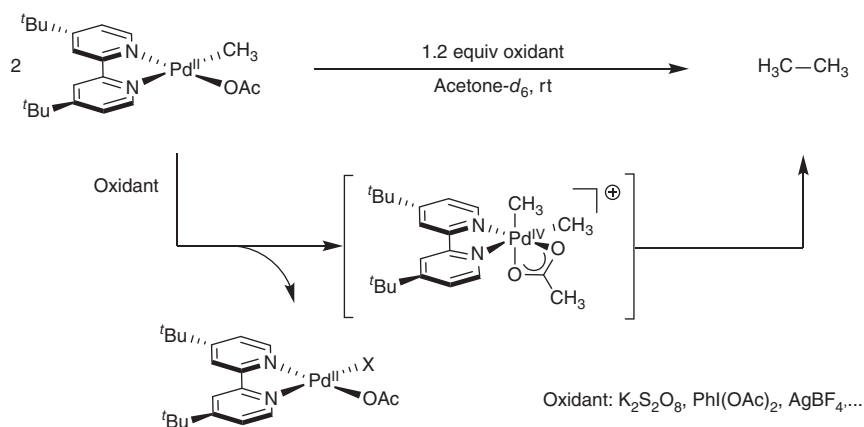


Figure 1.18 Ethane formation from palladium(II) complexes.

ambient conditions by employing practical metal catalysts [107]. Moreover, the recent development of electrocatalysis, which can enable single-electron transfer events without the need for a stoichiometric amount of oxidants or reductants, provides another powerful avenue for the direct C–H functionalization of methane under more atom economic and mild reaction conditions [108, 109].

As such, we anticipate that more and more direct conversions of methane will emerge in the near future. Catalytic transformations utilizing highly efficient catalysts under more economic and ecologically benign conditions will provide intriguing opportunities to exploit this C1 feedstock for more sustainable synthesis.

References

- 1 Wang, B., Albarracín-Suazo, S., Pagán-Torres, Y., and Nikolla, E. (2017). *Catal. Today* 285: 147–158.
- 2 Arutyunov, V.S. and Strekova, L.N. (2017). *J. Mol. Catal. A: Chem.* 426: 326–342.
- 3 Tang, P., Zhu, Q.J., Wu, Z.X., and Ma, D. (2014). *Energy Environ. Sci.* 7: 2580–2591.
- 4 Ma, S., Guo, X., Zhao, L. et al. (2013). *J. Energy Chem.* 22: 1–20.
- 5 Caballero, A. and Pérez, P.J. (2013). *Chem. Soc. Rev.* 42: 8809–8820.
- 6 Schwarz, H. (2011). *Angew. Chem. Int. Ed.* 50: 10096–10115.
- 7 Sun, L., Wang, Y., Guan, N., and Li, L. (2020). *Energy Technol.* 8: 1900826.
- 8 Havran, V., Duduković, M.P., and Lo, C.S. (2011). *Ind. Eng. Chem. Res.* 50: 7089–7100.
- 9 Gunsalus, N.J., Koppaka, A., Park, S.H. et al. (2017). *Chem. Rev.* 117: 8521–8573.
- 10 Schwach, P., Pan, X., and Bao, X. (2017). *Chem. Rev.* 117: 8497–8520.
- 11 Horn, R. and Schlögl, R. (2015). *Catal. Lett.* 145: 23–39.

- 12 Olivos-Suarez, A.I., Szécsényi, Á., Hensen, E.J.M. et al. (2016). *ACS Catal.* 6: 2965–2981.
- 13 Ravi, M., Ranocchiari, M., and van Bokhoven, J.A. (2017). *Angew. Chem. Int. Ed.* 56: 16464–16483.
- 14 Labinger, J.A. and Bercaw, J.E. (2002). *Nature* 417: 507–514.
- 15 Shilov, A.E. and Shteinman, A.A. (1977). *Coord. Chem. Rev.* 24: 97–143.
- 16 Periana, R.A., Taube, D.J., Gamble, S. et al. (1998). *Science* 280: 560–564.
- 17 Mironov, O.A., Bischof, S.M., Konnick, M.M. et al. (2013). *J. Am. Chem. Soc.* 135: 14644–14658.
- 18 Michalkiewicz, B., Ziebro, J., and Tomaszewska, M. (2006). *J. Membr. Sci.* 286: 223–227.
- 19 Zimmermann, T., Bilke, M., Soorholtz, M., and Schüth, F. (2018). *ACS Catal.* 8: 9262–9268.
- 20 Zimmermann, T., Soorholtz, M., Bilke, M., and Schüth, F. (2016). *J. Am. Chem. Soc.* 138: 12395–12400.
- 21 Palkovits, R., von Malotki, C., Baumgarten, M. et al. (2010). *ChemSusChem* 3: 277–282.
- 22 Dang, H.T., Lee, H.W., Lee, J. et al. (2018). *ACS Catal.* 8: 11854–11862.
- 23 Sen, A., Benvenuto, M.A., Lin, M. et al. (1994). *J. Am. Chem. Soc.* 116: 998–1003.
- 24 Periana, R.A., Taube, D.J., Evitt, E.R. et al. (1993). *Science* 259: 340–343.
- 25 Jones, C., Taube, D., Ziatdinov, V.R. et al. (2004). *Angew. Chem. Int. Ed.* 43: 4626–4629.
- 26 De Vos, D.E. and Sels, B.F. (2005). *Angew. Chem. Int. Ed.* 44: 30–32.
- 27 Kao, L.C., Hutson, A.C., and Sen, A. (1991). *J. Am. Chem. Soc.* 113: 700–701.
- 28 Gretz, E., Oliver, T.F., and Sen, A. (1987). *J. Am. Chem. Soc.* 109: 8109–8111.
- 29 Meyer, D., Taige, M.A., Zeller, A. et al. (2009). *Organometallics* 28: 2142–2149.
- 30 Muehlhofer, M., Strassner, T., and Herrmann, W.A. (2002). *Angew. Chem. Int. Ed.* 41: 1745–1747.
- 31 An, Z., Pan, X., Liu, X. et al. (2006). *J. Am. Chem. Soc.* 128: 16028–16029.
- 32 Basicke, N., Hogan, T.E., and Sen, A. (1996). *J. Am. Chem. Soc.* 118: 13111–13112.
- 33 Mukhopadhyay, S., Zerella, M., and Bell, A.T. (2005). *Adv. Synth. Catal.* 347: 1203–1206.
- 34 Yin, G., Piao, D.-g., Kitamura, T., and Fujiwara, Y. (2000). *Appl. Organomet. Chem.* 14: 438–442.
- 35 Ravi, M. and van Bokhoven, J.A. (2018). *ChemCatChem* 10: 2383–2386.
- 36 Schwartz, N.A., Boaz, N.C., Kalman, S.E. et al. (2018). *ACS Catal.* 8: 3138–3149.
- 37 Park, E.D., Hwang, Y.-S., Lee, C.W., and Lee, J.S. (2003). *Appl. Catal., A* 247: 269–281.
- 38 Yuan, Q., Deng, W., Zhang, Q., and Wang, Y. (2007). *Adv. Synth. Catal.* 349: 1199–1209.
- 39 Ohkubo, K. and Hirose, K. (2018). *Angew. Chem. Int. Ed.* 57: 2126–2129.
- 40 Zhang, L., Sun, Z., Lang, J., and Hu, Y.H. (2020). *Int. J. Energy Res.* <https://doi.org/10.1002/er.5948>.

- 41 Shteinman, A.A. (2020). *Kinet. Catal.* 61: 339–359.
- 42 Balasubramanian, R. and Rosenzweig, A.C. (2007). *Acc. Chem. Res.* 40: 573–580.
- 43 Baik, M.-H., Newcomb, M., Friesner, R.A., and Lippard, S.J. (2003). *Chem. Rev.* 103: 2385–2420.
- 44 Chen, M.M., Coelho, P.S., and Arnold, F.H. (2012). *Adv. Synth. Catal.* 354: 964–968.
- 45 Ito, H., Mori, F., Tabata, K. et al. (2014). *RSC Adv.* 4: 8645–8648.
- 46 Kim, H.J., Huh, J., Kwon, Y.W. et al. (2019). *Nat. Catal.* 2: 342–353.
- 47 Forster, D. (1979). Mechanistic pathways in the catalytic carbonylation of methanol by rhodium and iridium complexes. In: *Advances in Organometallic Chemistry*, vol. 17 (eds. F.C.A. Stone and R. West), 255–267. New York: Academic Press.
- 48 Lin, M. and Sen, A. (1992). *J. Chem. Soc., Chem. Commun.*: 892–893.
- 49 Nishiguchi, T., Nakata, K., Takaki, K., Fujiwara, Y. (1992). *Chem. Lett.* 21: 1141–1142.
- 50 Nakata, K., Yamaoka, Y., Miyata, T. et al. (1994). *J. Organomet. Chem.* 473: 329–334.
- 51 Asadullah, M., Taniguchi, Y., Kitamura, T., and Fujiwara, Y. (1998). *Sekiyu Gakkaishi* 41: 236–239.
- 52 Taniguchi, Y., Hayashida, T., Kitamura, T., and Fujiwara, Y. (1998). Vanadium-catalyzed acetic acid synthesis from methane and carbon dioxide. *Advances in Chemical Conversions for Mitigating Carbon Dioxide*, vol. 114 (eds. T. Inui, M. Anpo, K. Izui, et al.), 439–442. Elsevier.
- 53 Taniguchi, Y., Hayashida, T., Shibasaki, H. et al. (1999). *Org. Lett.* 1: 557–560.
- 54 Asadullah, M., Kitamura, T., and Fujiwara, Y. (1999). *Appl. Organomet. Chem.* 13: 539–547.
- 55 Asadullah, M., Taniguchi, Y., Kitamura, T., and Fujiwara, Y. (1999). *Tetrahedron Lett.* 40: 8867–8871.
- 56 Asadullah, M., Taniguchi, Y., Kitamura, T., and Fujiwara, Y. (2000). *Appl. Catal., A* 194: 443–452.
- 57 Asadullah, M., Kitamura, T., and Fujiwara, Y. (2000). *Angew. Chem. Int. Ed.* 39: 2475–2478.
- 58 Tsugio, K., Yusuke, I., Teizo, Y., and Yuzo, F. (2003). *Bull. Chem. Soc. Jpn.* 76: 1677–1678.
- 59 Zerella, M., Mukhopadhyay, S., and Bell, A.T. (2003). *Org. Lett.* 5: 3193–3196.
- 60 Wilcox, E.M., Roberts, G.W., and Spivey, J.J. (2002). *Appl. Catal., A* 226: 317–318.
- 61 Wilcox, E.M., Gogate, M.R., Spivey, J.J., and Roberts, G.W. (2001). Direct synthesis of acetic acid from methane and carbon dioxide. *Natural Gas Conversion VI. Stud. Surf. Sci. Catal.*, vol. 136 (eds. E. Iglesia, J.J. Spivey and T.H. Fleisch), 259–264. Elsevier.
- 62 Reis, P.M., Silva, J.A.L., Palavra, A.F. et al. (2003). *Angew. Chem. Int. Ed.* 42: 821–823.
- 63 Kirillova, M.V., da Silva, J.A.L., Fraústo da Silva, J.J.R., and Pombeiro, A.J.L. (2007). *Appl. Catal., A* 332: 159–165.

- 64 Kirillova, M.V., Kuznetsov, M.L., Reis, P.M. et al. (2007). *J. Am. Chem. Soc.* 129: 10531–10545.
- 65 Lin, M. and Sen, A. (1994). *Nature* 368: 613.
- 66 Kurika, M., Nakata, K., Jintoku, T., Taniguchi, Y., Takaki, K., Fujiwara, Y. (1995). *Chem. Lett.* 24: 244–244.
- 67 Lin, M., Hogan, T.E., and Sen, A. (1996). *J. Am. Chem. Soc.* 118: 4574–4580.
- 68 Chepaikin, E.G., Boyko, G.N., Bezruchenko, A.P. et al. (1998). *J. Mol. Catal. A: Chem.* 129: 15–18.
- 69 Chepaikin, E.G., Bezruchenko, A.P., Leshcheva, A.A. et al. (2001). *J. Mol. Catal. A: Chem.* 169: 89–98.
- 70 Nizova, G.V., Suss-Fink, G., Stanislas, S., and Shul'pin, G.B. (1998). *Chem. Commun.*: 1885–1886.
- 71 Yuan, J., Liu, L., Wang, L., and Hao, C. (2013). *Catal. Lett.* 143: 126–129.
- 72 Periana, R.A., Mironov, O., Taube, D. et al. (2003). *Science* 301: 814–818.
- 73 Periana, R.A., Mironov, O., Taube, D. et al. (2005). *Top. Catal.* 32: 169–174.
- 74 Zerella, M., Mukhopadhyay, S., and Bell, A.T. (2004). *Chem. Commun.*: 1948–1949.
- 75 Zerella, M., Kahros, A., and Bell, A. (2006). *J. Catal.* 237: 111–117.
- 76 Zerella, M. and Bell, A.T. (2006). *J. Mol. Catal. A: Chem.* 259: 296–301.
- 77 Hogeveen, H., Lukas, J., and Roobeek, C.F. (1969). *J. Chem. Soc. D:* 920–921.
- 78 Bagno, A., Bukala, J., and Olah, G.A. (1990). *J. Org. Chem.* 55: 4284–4289.
- 79 de Rege, P.J.F., Gladysz, J.A., and Horváth, I.T. (2002). *Adv. Synth. Catal.* 344: 1059–1062.
- 80 Asadullah, M., Taniguchi, Y., Kitamura, T., and Fujiwara, Y. (1998). *Appl. Organomet. Chem.* 12: 277–284.
- 81 Gernon, M.D., Wu, M., Buszta, T., and Janney, P. (1999). *Green Chem.* 1: 127–140.
- 82 Lobree, L.J. and Bell, A.T. (2001). *Ind. Eng. Chem. Res.* 40: 736–742.
- 83 Mukhopadhyay, S. and Bell, A.T. (2003). *Angew. Chem. Int. Ed.* 42: 2990–2993.
- 84 Mukhopadhyay, S. and Bell, A.T. (2003). *Angew. Chem. Int. Ed.* 42: 1019–1021.
- 85 Msukhopadhyay, S. and Bell, A.T. (2003). *Org. Process Res. Dev.* 7: 161–163.
- 86 Mukhopadhyay, S. and Bell, A.T. (2004). *J. Mol. Catal. A: Chem.* 211: 59–65.
- 87 Mukhopadhyay, S. and Bell, A.T. (2004). *Adv. Synth. Catal.* 346: 913–916.
- 88 Mukhopadhyay, S. and Bell, A.T. (2003). *J. Am. Chem. Soc.* 125: 4406–4407.
- 89 Mukhopadhyay, S. and Bell, A.T. (2003). *Chem. Commun.*: 1590–1591.
- 90 Shaabani, A. and Ghadari, R. (2010). *Ind. Eng. Chem. Res.* 49: 7685–7686.
- 91 Díaz-Urrutia, C. and Ott, T. (2019). *Science* 363: 1326–1329.
- 92 Lennox, A.J.J. and Lloyd-Jones, G.C. (2014). *Chem. Soc. Rev.* 43: 412–443.
- 93 Cook, A.K., Schimler, S.D., Matzger, A.J., and Sanford, M.S. (2016). *Science* 351: 1421–1424.
- 94 Smith, K.T., Berritt, S., González-Moreiras, M. et al. (2016). *Science* 351: 1424–1427.
- 95 Ahn, S., Sorsche, D., Berritt, S. et al. (2018). *ACS Catal.* 8: 10021–10031.
- 96 Trowbridge, A., Walton, S.M., and Gaunt, M.J. (2020). *Chem. Rev.* 120: 2613–2692.

- 97 Hu, A., Guo, J.-J., Pan, H., and Zuo, Z. (2018). *Science* 361: 668–672.
- 98 Gunsalus, N.J., Park, S.H., Hashiguchi, B.G. et al. (2019). *Organometallics* 38: 2319–2322.
- 99 Caballero, A., Despagnet-Ayoub, E., Mar Díaz-Requejo, M. et al. (2011). *Science* 332: 835–838.
- 100 Fuentes, M.Á., Olmos, A., Muñoz, B.K. et al. (2014). *Chem. Eur. J.* 20: 11013–11018.
- 101 Gava, R., Olmos, A., Noverges, B. et al. (2015). *ACS Catal.* 5: 3726–3730.
- 102 Laudadio, G., Deng, Y., van der Wal, K. et al. (2020). *Science* 369: 92–96.
- 103 Lotz, M.D., Remy, M.S., Lao, D.B. et al. (2014). *J. Am. Chem. Soc.* 136: 8237–8242.
- 104 Cheng, H., Wang, X., Chang, L. et al. (2019). *Sci. Bull.* 64: 1896–1901.
- 105 Prier, C.K., Rankic, D.A., and MacMillan, D.W.C. (2013). *Chem. Rev.* 113: 5322–5363.
- 106 Romero, N.A. and Nicewicz, D.A. (2016). *Chem. Rev.* 116: 10075–10166.
- 107 Meng, X., Cui, X., Rajan, N.P. et al. (2019). *Chem* 5: 2296–2325.
- 108 Natinsky, B.S., Lu, S.T., Copeland, E.D. et al. (2019). *ACS Cent. Sci.* 5: 1584–1590.
- 109 Kim, R.S. and Surendranath, Y. (2019). *ACS Cent. Sci.* 5: 1179–1186.